



Summary  
10 March 2020

## Radiative neutrino and radiative Bhabha cross section calculation tests.

J-J. Blaising <sup>‡</sup>

<sup>‡</sup>.

### Abstract

At  $e^+e^-$  colliders, Weakly Interacting Massive Particles (WIMPs), can be searched for using as tag particle a photon from initial state radiation. The main backgrounds for this search are:  $e^+e^- \rightarrow \nu \bar{\nu} \gamma$  ( $\gamma$ ) and  $e^+e^- \rightarrow e^+e^- \gamma$  ( $\gamma$ ). At LEP all four experiments used the program KKMC to compute the cross-section of the radiative neutrino process and the program TEEG to compute the cross-section of the radiative Bhabha process. At CLIC the WHIZARD program is used to compute the cross-sections of these processes. To test WHIZARD, radiative neutrino and radiative Bhabha cross-sections are computed at 91.2 GeV and 207 GeV and compared with the cross sections measured by the L3 LEP experiment or with the expected cross-section computed using KKMC or TEEG.

## 1 Introduction

At  $e^+e^-$  colliders, WIMPs are searched for using as signature a photon from initial state radiation and missing energy. Searches for single and multi-photon final states with missing energy have been performed by LEP experiments [1], [2] [3], [4]. All details about the L3 analysis can be found in the PhD of M.I.Gataullin [5]. The main backgrounds for this search are:  $e^+e^- \rightarrow \nu \bar{\nu} \gamma (\gamma)$  and  $e^+e^- \rightarrow e^+e^- \gamma (\gamma)$ . The WHIZARD program [6], is used to compute the radiative neutrino cross-section at 91.2 GeV and 207 GeV. The expected cross sections are compared with the cross sections measured by the L3 LEP experiment and to the expected cross-section computed using the KKMC program [7]. At LEP the four experiments used the program TEEG [8] to compute the cross sections of the process  $e^+e^- \rightarrow e^+e^- \gamma (\gamma)$ . The radiative Bhabha cross-section computed at 207 GeV using WHIZARD is compared with the expected value reported in table 6.2 of the PhD of M.I.Gataullin [5].

## 2 L3 cross sections at 91.2 GeV and 207 GeV

L3 selection cuts and cross-section value of the process  $e^+e^- \rightarrow \nu \bar{\nu} \gamma (\gamma)$  at  $\sqrt{s} = 91.2$  GeV and  $\sqrt{s} = 207$  GeV are given in [9] and [3] respectively. Table 1 shows the selection cuts and the cross-section value at  $\sqrt{s} = 91.2$  GeV.

Table 1: L3 selection cuts and cross-section value at  $\sqrt{s} = 91.2$  [GeV]

Process	Cuts	$\sigma$ [pb]
$e^+e^- \rightarrow \nu \bar{\nu} \gamma (\gamma)$	$45^\circ < \theta_\gamma < 135^\circ$ and $1 \text{ GeV} < E_\gamma < 10 \text{ GeV}$	$29.4 \pm 1.3$

Table 2 shows the selection cuts and cross-section value of the process  $e^+e^- \rightarrow \nu \bar{\nu} \gamma (\gamma)$  at  $\sqrt{s} = 207$  GeV. The table shows also the expected cross-section computed with KKMC.

Table 2: L3  $\nu \bar{\nu} \gamma (\gamma)$  selection cuts, measured cross-section and expected cross-section at  $\sqrt{s} = 207$  [GeV]

Process	Cuts	measured $\sigma$ [pb]	expected $\sigma$ [pb]
$e^+e^- \rightarrow \nu \bar{\nu} \gamma (\gamma)$	$14^\circ < \theta_\gamma < 166^\circ$ and $Pt_\gamma/\sqrt{s} > 0.02$	$4.0 \pm 0.21$	4.15

Table 3 shows the L3 selection cuts and expected cross section value computed using TEEG  $\sqrt{s} = 207$  GeV.

Table 3: L3 selection cuts and expected TEEG cross section value at  $\sqrt{s} = 207$  [GeV]

Process	Cuts	$\sigma$ [pb]
$e^+e^- \rightarrow e^+e^- \gamma (\gamma)$	$13.5^\circ < \theta_\gamma < 166.5^\circ$ and $E_\gamma > 0.9 \text{ GeV}$ $\theta_e < 11^\circ$	174

## 3 WHIZARD cross sections at 380 GeV

The beam conditions at CLIC are different from the LEP beam conditions. At CLIC the beam spectrum (BS) has to be taken into account. At CLIC and LEP initial state radiation (ISR) has to be taken into account. In Whizard the initial state radiation can be applied without or with recoil. Using the recoil gives  $Pt$  to the isr photon. The beam and initial state radiation conditions, BS, ISR, RECOIL, lead to different cross section values depending on the combination of these conditions. Each of the three conditions BS, ISR, RECOIL can be true (T) or false (F). The cross sections were thus computed for the 6 different

beam and isr conditions: FFF, FTF, FTT, TFF, TTF, TTT. To test WHIZARD different observables were also computed. For the radiative neutrino process:

- Incoming beam electron mass  $me_{in}^- = \sqrt{E^2 - P^2}$
- Incoming beam positron mass  $me_{in}^+ = \sqrt{E^2 - P^2}$
- $M(e_{in}^-, \gamma)$
- $M(e_{in}^+, \gamma)$

For the radiative Bhabha process:

- Incoming beam electron mass  $me_{in}^- = \sqrt{E^2 - P^2}$
- Outgoing beam electron mass  $me_{out}^- = \sqrt{E^2 - P^2}$
- $M(e_{in}^-, e_{out}^-)$
- $M(e_{in}^+, e_{out}^+)$

For the combinations FTT (ISR, RECOIL), TFF (BS) and TTT (BS, ISR, RECOIL)  $me_{in}^- = 0$  and  $me_{in}^+ = 0$ . Table 4 shows, for the radiative neutrino process, the experimental cut values, the WHIZARD cuts to control the divergence  $-M(e^\pm, \gamma_m) < -me$ , the ISR cuts and the cross section values. The cuts to control the divergence are applied on the matrix element photons labeled  $\gamma_m$ . The cuts avoiding overlapping of isr photons with matrix element photons are applied on the isr photons labeled  $\gamma_i$ . For the radiative neutrino

Table 4: Radiative neutrino cross section values [pb] at  $\sqrt{s} = 380$  [GeV]

Experimental Cuts	Whizard Cuts	Beam Conditions					
		FFF	FTF	FTT	TFF	TTF	TTT
$7^\circ < \theta_{\gamma_m} < 173^\circ$ and $Pt_{\gamma_m} > 5$ GeV	No	3.02	3.18	3.18	3.04	3.21	3.21
	$-M(e^\pm, \gamma_m) < -me$	3.02	3.18	3.18	3.04	3.21	3.21
	$\theta_{\gamma_i} < 7^\circ$ or $Pt_{\gamma_i} < 5$ GeV			2.98			3.01

process with one matrix element photon there is no cross-section computing issue  $-M(e, \gamma) \ll -me$ . The cuts avoiding overlapping of isr photons with matrix element photons is reducing the cross-section value by 6%.

Table 5 shows, for the radiative Bhabha process, the experimental cut values, the WHIZARD cut to control the divergence  $-M(e_{in}^\pm, e_{out}^\mp) < -me \times \sqrt{2}$ , the ISR cuts and the cross section values. The cuts avoiding overlapping of isr photons with matrix element photons are applied on the isr photons labeled  $\gamma_i$ . For the radiative Bhabha process with one matrix element photon the cut  $-M(e_{in}^\pm, e_{out}^\mp) < me \times \sqrt{2}$

Table 5: Radiative Bhabha cross section values [pb] at  $\sqrt{s} = 380$  [GeV]

Experimental Cuts	Whizard Cuts	Beam Conditions					
		FFF	FTF	FTT	TFF	TTF	TTT
$7^\circ < \theta_{\gamma_m} < 173^\circ$ and $Pt_{\gamma_m} > 5$ GeV	No	179	193	193	461	201	202
	$-M(e_{in}^\pm, e_{out}^\mp) < -me \times \sqrt{2}$	144	156	156	150	163	163
	$\theta_{\gamma_i} < 7^\circ$ or $Pt_{\gamma_i} < 5$ GeV			145			153

controls the divergence which is most important for the condition TFF.

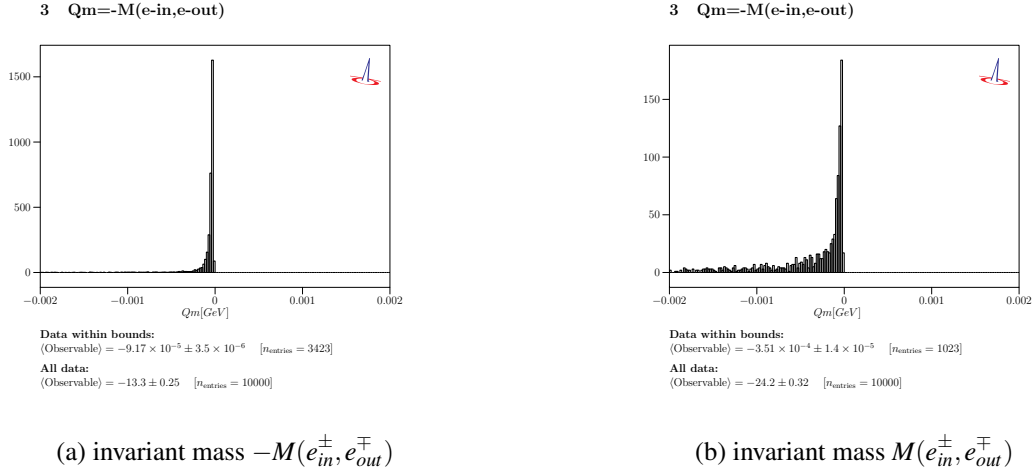


Figure 1:  $e^+ e^- \rightarrow e^+ e^- \gamma$  at  $\sqrt{s} = 380$  GeV; invariant mass  $M(e_{in}^{\pm}, e_{out}^{\mp})$  (a) for beam spectrum only (b) for beam spectrum, isr and recoil

Figure 1(a) and Figure 1(b) show the invariant mass  $-M(e_{in}^{\pm}, e_{out}^{\mp})$ , for the radiative Bhabha process, for the condition BS only and for the condition (BS,ISR,RECOIL) respectively. The number of events within the histogram bound is 3.4 times larger for the TFF condition with respect to the TTT condition. Adding isr photons with recoil is reducing the effect of the divergence.

## 4 Whizard cross sections at 91.2 GeV and 207 GeV

Table 6 shows, for the radiative neutrino process, the experimental cut values, the WHIZARD cuts to control the divergence  $-M(e^{\pm}, \gamma_m) < -me$ , the ISR cuts and the cross section values. The cuts to control the divergence are applied on the matrix element photons labeled  $\gamma_m$ . The cuts avoiding overlapping of isr photons with matrix element photons are applied on the isr photons labeled  $\gamma_i$ .

Table 6: Radiative neutrino cross section values [pb] at  $\sqrt{s} = 91.2$  [GeV]

Experimental Cuts	Whizard Cuts	Beam Conditions		
		FFF	FTF	FTT
$45^\circ < \theta_{\gamma_m} < 135^\circ$ and $1 \text{ GeV} < E_{\gamma_m} < 10 \text{ GeV}$	No	42.01	29.61	29.61
	$-M(e^{\pm}, \gamma_m) < -me$	42.01	29.61	29.61
	$\theta_{\gamma_i} < 45^\circ$ or $E_{\gamma_i} < 1 \text{ GeV}$			29.60

For the radiative neutrino process there is a good agreement between the WHIZARD cross section 29.6 pb and the L3 measured value  $29.4 \pm 1.3$  pb.

Table 7 shows, for the radiative neutrino process, the experimental cut values, the WHIZARD cuts to control the divergence  $-M(e^{\pm}, \gamma_m) < -me$ , the ISR cuts and the cross section values. The cuts to control the divergence are applied on the matrix element photons labeled  $\gamma_m$ . The cuts avoiding overlapping of isr photons with matrix element photons are applied on the isr photons labeled  $\gamma_i$ .

For the radiative neutrino process there is a good agreement between the WHIZARD cross section 4.12 pb and the L3 measured value  $4.0 \pm 0.2$  pb and the expected value computed with KKMC is 4.15 pb.

Table 8 shows, for the radiative Bhabha process, the experimental cut values, the WHIZARD cuts

Table 7: Radiative neutrino cross section values [pb] at  $\sqrt{s} = 207$  [GeV]

Experimental Cuts	Whizard Cuts	Beam Conditions		
		FFF	FTF	FTT
$14^\circ < \theta_{\gamma_m} < 166^\circ$ and $Pt_{\gamma_m}/\sqrt{s} > 0.02$	No	3.77	4.38	4.38
	$-M(e^\pm, \gamma_m) < -me$	3.77	4.38	4.38
	$\theta_{\gamma_i} < 14^\circ$ or $Pt_{\gamma_i}/\sqrt{s} > 0.02$			4.12

to control the divergence  $M(e_{in}^\pm, e_{out}^\mp) < me \times \sqrt{2}$ , the ISR cuts and the cross section values. The cuts to control the divergence are applied on the matrix element photons labeled  $\gamma_m$ . The cuts avoiding overlapping of isr photons with matrix element photons are applied on the isr photons labeled  $\gamma_i$ .

Table 8: Radiative Bhabha cross section values [pb] at  $\sqrt{s} = 207$  [GeV]

Experimental Cuts	Whizard Cuts	Beam Conditions		
		FFF	FTF	FTT
$13.5^\circ < \theta_{\gamma_m} < 166.5^\circ$ and $E_{\gamma_m} > 0.9$ GeV and $\theta_e < 11^\circ$	No	250	326	326
	$-M(e_{in}^\pm, e_{out}^\mp) < -me \times \sqrt{2}$	157	202	202
	$\theta_{\gamma_i} < 13.5^\circ$ or $E_{\gamma_i} < 0.9$ GeV			181

With the cut  $-M(e_{in}^\pm, e_{out}^\mp) < -me \times \sqrt{2}$  the cross-section is 181 pb. Changing the cut to  $-M(e_{in}^\pm, e_{out}^\mp) < -me \times 2$  leads to a cross-section of 175 pb. For the radiative Bhabha process there is a good agreement between the WHIZARD cross section and the expected value computed with TEEG 174 pb.

## 5 Summary

Using invariant mass cuts allows controlling the divergence when computing the cross-sections of radiative neutrino and radiative Bhabha processes. At  $\sqrt{s} = 91.2$  GeV, for the process  $e^+ e^- \rightarrow \nu \bar{\nu} \gamma$  ( $\gamma$ ) the beam option FTT gives an expected cross section in good agreement with the cross section measured by L3 experiment,

At  $\sqrt{s} = 207$  [GeV] for the process  $e^+ e^- \rightarrow \nu \bar{\nu} \gamma$  ( $\gamma$ ), the beam option FTT gives an expected cross section in good agreement with the measured cross section and with the expected value computed with KKMC. For the process  $e^+ e^- \rightarrow e^+ e^- \gamma$  ( $\gamma$ ) at  $\sqrt{s} = 207$  [GeV] the beam option FTT gives an expected cross section which is close to the expected value computed using TEEG.

## References

- [1] A. Heister, et al.(ALEPH Collaboration),  
*Single photon and multiphoton production in  $e^+e^-$  collisions at  $\sqrt{s}$  up to 209 GeV*,  
Eur.Phys.J. **C28** (2003) 1.
- [2] J. Abdallah, et al.(DELPHI Collaboration),  
*Photon events with missing energy in  $e^+e^-$  collisions at  $\sqrt{s} = 130$  GeV to 209 GeV*,  
Eur.Phys.J. **C38** (2005) 395.
- [3] P. Achard, et al.(L3 Collaboration),  
*Single photon and multiphoton events with missing energy in  $e^+e^-$  collisions at LEP*,  
Phys. Lett. **B587** (2004) 16.

- 
- [4] G. Abbiendi, et al.(OPAL Collaboration),  
*Photonic events with missing energy in  $e^+e^-$  collisions at  $\sqrt{s} = 189$  GeV*,  
Eur.Phys.J. **C18** (2000) 253.
- [5] M. I. Gataullin, *Studies of electroweak interactions and searches for new physics using photonic events with missing energy at the Large Electron-Positron Collider*. 2006, DOI: [10.7907/V4BM-7H20](https://doi.org/10.7907/V4BM-7H20).<https://resolver.caltech.edu/CaltechETD:etd-01202006-052920>.
- [6] W. Kilian, T. Ohl, J. Reuter, *WHIZARD: Simulating Multi-Particle Processes at LHC and ILC*,  
Eur.Phys.J. **C71** (2011) 1742, DOI: [arXiv:0708.4233](https://arxiv.org/abs/0708.4233) [hep-ph].
- [7] B. Jadach S. Ward, Z. Was, *KKMC*, Phys.Rev **D63** (2001) 113009.
- [8] D. Karlen, *Radiative Bhabha Scattering For Singly Tagged And Untagged Configurations*,  
Nuclear. Physics. **B289** (1987) 23.
- [9] M. Acciari, et al.(L3 Collaboration),  
*Determination of the Number of Light Neutrino Species from Single Photon Production at LEP*,  
Phys. Lett. **B431** (1998) 199.